An analytical solution to electromagnetic multisphere-scattering

—— the scattering formulation used in codes gmm01f.f and gmm01s.f

Yu-lin Xu and Bo Å. S. Gustafson

Department of Astronomy, P.O.Box 112055, University of Florida, Gainesville, FL 32611-2055

1. Introduction

Electromagnetic scattering by small particles is an important subject in a surprisingly wide range of scientific and technical fields. For a long time, analytical solutions exist only for a few types of highly symmetric geometries of single scatterers. Small particles in nature, however, often have an aggregate structure of complex morphology. Due to two fundamental multiple scattering effects — interaction and interference, electromagnetic multiparticle-scattering and its theoretical description possess distinguishing features, in comparison with single-particle scattering. The development of addition theorems for vector spherical wave functions (VSWF) made it feasible to tackle multiparticle light-scattering problems analytically.[1,2] Starting with the pioneer work by Liang and Lo[3] and Bruning and Lo,[4] researchers have made substantial efforts to develop a rigorous multisphere scattering solution.[5,6] This note briefly summarizes an analytical far-field solution to electromagnetic scattering by an aggregate of spheres in a fixed orientation,[7–11] which is implemented in the code gmm01f.f. It is an extension of Mie theory[12–14] to the multisphere case and referred to as the Generalized Multiparticle Mie-solution (GMM).[15]

2. Expansion of incident plane wave in displaced coordinate systems

Fortran codes gmm01f.f and gmm01s.f calculate the scattering of a monochromatic plane wave by an aggregate of nonintersecting, homogeneous spheres in a fixed orientation or at an average over individual orientations. (Code gmm01s.f and gmm01f.f differ only in the computer-memory requirement. The gmm01s.f code is slower than gmm01f.f but can handle a very large number of component particles that gmm01f.f is unable to handle.) The aggregate is embedded in a non-absorbing homogeneous medium characterized by dielectric constant ε_0 and permeability μ_0. Scattered fields from each individual spheres are solved in respective sphere-centered reference systems. In an arbitrarily chosen primary j_0th coordinate system, the Cartesian coordinates of the origins of these L displaced coordinate systems (i.e., the sphere-centers) are (X^j, Y^j, Z^j), $j = 1, 2, \ldots, L$. Without loss of generality, the incident plane wave vector always points to the positive z direction.

To solve multisphere-scattering through the Mie-type multipole superposition approach, the incident plane wave is expanded in terms of VSWF in each of the L sphere-centered coordinate systems. A z-propagating plane wave with a linear polarization angle $\beta_{\rm p}$ is characterized by the wave vector $\mathbf{k} = k\hat{\mathbf{e}}_z$, where $k = 2\pi/\lambda$ is the wave number, λ is the incident wavelength in the surrounding medium, and $\hat{\mathbf{e}}_z$ together with $\hat{\mathbf{e}}_x, \hat{\mathbf{e}}_y$ are the orthonormal unit vectors in the Cartesian coordinate system. In the primary j_0th coordinate system, the incident electric field vector is

$$\mathbf{E}_{\rm inc} = \mathbf{E_0} \exp(ikz), \tag{1}$$

where $\mathbf{E_0} = E_0(\hat{\mathbf{e}}_x \cos\beta_\mathrm{p} + \hat{\mathbf{e}}_y \sin\beta_\mathrm{p})$ and $i = \sqrt{-1}$. The harmonic time term $\exp(-i\omega t)$ is suppressed, where ω is the circular frequency. In the j_0th coordinate system, the incident electromagnetic field can be expanded in VSWF as follows:

$$\mathbf{E}_\mathrm{inc} = -\sum_{n=0}^{N}\sum_{m=-n}^{n} iE_{mn}\Big[p_{mn}\mathbf{N}_{mn}^{(1)}(\rho,\theta,\phi) + q_{mn}\mathbf{M}_{mn}^{(1)}(\rho,\theta,\phi)\Big], \tag{2a}$$

$$\mathbf{H}_\mathrm{inc} = -\frac{k}{\omega\mu_0}\sum_{n=0}^{N}\sum_{m=-n}^{n} E_{mn}\Big[q_{mn}\mathbf{N}_{mn}^{(1)}(\rho,\theta,\phi) + p_{mn}\mathbf{M}_{mn}^{(1)}(\rho,\theta,\phi)\Big], \tag{2b}$$

where $\rho = kr$ and

$$E_{mn} = E_0 i^n \left[\frac{(2n+1)}{n(n+1)}\frac{(n-m)!}{(n+m)!}\right]^{1/2}. \tag{3}$$

It needs to mention here that the normalization factor E_{mn} defined by Eq. (3) is different from the one previously used,[7–11,15] which was

$$E_{mn} = E_0 i^n (2n+1)\frac{(n-m)!}{(n+m)!}. \tag{4}$$

Consequently, the constant factors in the scattering formulas summarized here and used in gmm01f.f are different from those found in the references. Vector spherical wave functions $\mathbf{M}_{mn}^{(1)}$ and $\mathbf{N}_{mn}^{(1)}$ have a specific component form

$$\mathbf{M}_{mn}^{(1)}(\rho,\theta,\phi) = \Big[\hat{\mathbf{e}}_\theta i\pi_{mn}(\cos\theta) - \hat{\mathbf{e}}_\phi \tau_{mn}(\cos\theta)\Big] j_n(\rho)\exp(im\phi), \tag{5a}$$

$$\begin{aligned}\mathbf{N}_{mn}^{(1)}(\rho,\theta,\phi) = &\Big\{\hat{\mathbf{e}}_r n(n+1)P_n^m(\cos\theta)\frac{j_n(\rho)}{\rho} \\ &+ \Big[\hat{\mathbf{e}}_\theta \tau_{mn}(\cos\theta) + \hat{\mathbf{e}}_\phi i\pi_{mn}(\cos\theta)\Big]\frac{\psi_n'(\rho)}{\rho}\Big\}\exp(im\phi),\end{aligned} \tag{5b}$$

where $\hat{\mathbf{e}}_r, \hat{\mathbf{e}}_\theta, \hat{\mathbf{e}}_\phi$ are the orthonormal basis vectors in the spherical coordinate system, j_n is the spherical Bessel function of the first kind, P_n^m is the associated Legendre function of the first kind, $\psi_n(\rho) = \rho j_n(\rho)$ is one of the Riccati-Bessel functions, a prime indicates the derivative of a function with respect to its argument, and

$$\pi_{mn}(\cos\theta) = \frac{m}{\sin\theta}P_n^m(\cos\theta), \tag{6a}$$

$$\tau_{mn}(\cos\theta) = \frac{\mathrm{d}}{\mathrm{d}\theta}P_n^m(\cos\theta). \tag{6b}$$

The definition used here for the associated Legendre function P_n^m follows the convention without the modulus $(-1)^m$. From Eqs. (1-3), (5), (6), and the orthogonality of VSWF, it follows that the primary expansion coefficients in Eqs. (2) are given by

$$p_{mn} = \frac{i\int_0^{2\pi}\int_0^{\pi}\exp(ikz)\mathbf{E_0}\cdot\mathbf{N}_{mn}^{(1)*}(\rho,\theta,\phi)\sin\theta\mathrm{d}\theta\mathrm{d}\phi}{E_{mn}\int_0^{2\pi}\int_0^{\pi}|\mathbf{N}_{mn}^{(1)}(\rho,\theta,\phi)|^2\sin\theta\mathrm{d}\theta\mathrm{d}\phi}, \tag{7a}$$

$$q_{mn} = \frac{i\int_0^{2\pi}\int_0^{\pi}\exp(ikz)\mathbf{E_0}\cdot\mathbf{M}_{mn}^{(1)*}(\rho,\theta,\phi)\sin\theta\mathrm{d}\theta\mathrm{d}\phi}{E_{mn}\int_0^{2\pi}\int_0^{\pi}|\mathbf{M}_{mn}^{(1)}(\rho,\theta,\phi)|^2\sin\theta\mathrm{d}\theta\mathrm{d}\phi}, \tag{7b}$$

which result in

$$p_{mn} = q_{mn} = 0, \qquad |m| \neq 1, \tag{8a}$$

$$p_{1n} = q_{1n} = \frac{\sqrt{2n+1}}{2} \exp(-i\beta_{\rm p}), \tag{8b}$$

$$p_{-1n} = -q_{-1n} = -\frac{\sqrt{2n+1}}{2} \exp(i\beta_{\rm p}). \tag{8c}$$

Note that these results are different from those given in previous works due to the change in normalization factor E_{mn}. In any displaced jth coordinate system centered on the jth sphere, the expansion of the incident field has the same form as Eqs. (2),

$$\mathbf{E}_{\rm inc}^{j} = \mathbf{E}_{\rm inc} = -\sum_{n=0}^{N^j} \sum_{m=-n}^{n} iE_{mn} \Big[p_{mn}^{j} \mathbf{N}_{mn}^{(1)}(\rho^j, \theta^j, \phi^j) + q_{mn}^{j} \mathbf{M}_{mn}^{(1)}(\rho^j, \theta^j, \phi^j) \Big], \tag{9a}$$

$$\mathbf{H}_{\rm inc}^{j} = \mathbf{H}_{\rm inc} = -\frac{k}{\omega\mu_0} \sum_{n=0}^{N^j} \sum_{m=-n}^{n} E_{mn} \Big[q_{mn}^{j} \mathbf{N}_{mn}^{(1)}(\rho^j, \theta^j, \phi^j) + p_{mn}^{j} \mathbf{M}_{mn}^{(1)}(\rho^j, \theta^j, \phi^j) \Big], \tag{9b}$$

where $\rho^j = kr^j$. Because $z^j = z - Z^j$, the incident electric field can also be written as $\mathbf{E}_{\rm inc}^{j} = \mathbf{E}_{\rm inc} = \mathbf{E_0} \exp(ikZ^j) \exp(ikz^j)$. A constant phase term $\exp(ikZ^j)$ is attached to the origin of the jth coordinate system. This assures that, described in the jth coordinate system, the incident field does not change the reference center for phase, which is always the origin of the primary coordinate system. The expansion coefficients of the incident field in Eqs. (9) are thus given by

$$p_{mn}^{j} = \exp(ikZ^j) p_{mn}, \qquad q_{mn}^{j} = \exp(ikZ^j) q_{mn}, \tag{10}$$

which differ from the primary expansion coefficients only by a simple, constant phase term.

3. Partial scattered fields of individual spheres

Similar to the incident field, individual scattered fields of each component spheres can be expanded in VSWF in respective sphere-centered coordinate systems,

$$\mathbf{E}_{\rm sca}^{l} = \sum_{n=1}^{N^l} \sum_{m=-n}^{n} iE_{mn} \left[a_{mn}^{l} \mathbf{N}_{mn}^{(3)}(\rho^l, \theta^l, \phi^l) + b_{mn}^{l} \mathbf{M}_{mn}^{(3)}(\rho^l, \theta^l, \phi^l) \right], \tag{11a}$$

$$\mathbf{H}_{\rm sca}^{l} = \frac{k}{\omega\mu_0} \sum_{n=1}^{N^l} \sum_{m=-n}^{n} E_{mn} \left[b_{mn}^{l} \mathbf{N}_{mn}^{(3)}(\rho^l, \theta^l, \phi^l) + a_{mn}^{l} \mathbf{M}_{mn}^{(3)}(\rho^l, \theta^l, \phi^l) \right], \tag{11b}$$

where $\mathbf{M}_{mn}^{(3)}$ and $\mathbf{N}_{mn}^{(3)}$ differ from $\mathbf{M}_{mn}^{(1)}$ and $\mathbf{N}_{mn}^{(1)}$ only in the generating function, which is $h_n^{(1)}$, the spherical Hankel function of the first kind, instead of j_n, the spherical Bessel function of the first kind. Solving boundary conditions for partial scattering coefficients (a_{mn}^l, b_{mn}^l) for all component spheres consists of the first concrete step toward a complete multisphere scattering solution. The solution of standard electromagnetic boundary conditions imposed on the spherical surface of a "detached" component sphere gives rise to[7]

$$a_{mn}^{l} = \bar{a}_n^l P_{mn}^{l}, \qquad b_{mn}^{l} = \bar{b}_n^l Q_{mn}^{l}, \tag{12}$$

where $\bar{a}_n^l$ and $\bar{b}_n^l$ are the Mie scattering coefficients of the isolated lth sphere. P_{mn}^l and Q_{mn}^l are the expansion coefficients of the total incident field for the lth sphere given by[7]

$$P_{mn}^l = p_{mn}^l - \sum_{j \neq l}^{(1,L)} \sum_{\nu=1}^{N^j} \sum_{\mu=-\nu}^{\nu} (A_{mn\mu\nu}^{jl} a_{\mu\nu}^j + B_{mn\mu\nu}^{jl} b_{\mu\nu}^j), \tag{13a}$$

$$Q_{mn}^l = q_{mn}^l - \sum_{j \neq l}^{(1,L)} \sum_{\nu=1}^{N^j} \sum_{\mu=-\nu}^{\nu} (B_{mn\mu\nu}^{jl} a_{\mu\nu}^j + A_{mn\mu\nu}^{jl} b_{\mu\nu}^j), \tag{13b}$$

where $A_{mn\mu\nu}^{jl}$ and $B_{mn\mu\nu}^{jl}$ are vector translation coefficients[1,2] characterizing the transformation of scattered waves from the jth sphere into incident waves for the lth sphere. The total electromagnetic field incident upon a component sphere in an aggregate consists of two parts: (1) the initial incident plane wave and (2) scattered waves from all other spheres in the aggregate. Equations (12) and (13) involve partial scattered fields from all interacting spheres and establish the large-dimensional linear system containing unknown partial scattering coefficients of all component spheres:

$$a_{mn}^l / \bar{a}_n^l + \sum_{j \neq l}^{(1,L)} \sum_{\nu=1}^{N^j} \sum_{\mu=-\nu}^{\nu} (A_{mn\mu\nu}^{jl} a_{\mu\nu}^j + B_{mn\mu\nu}^{jl} b_{\mu\nu}^j) = p_{mn}^l, \tag{14a}$$

$$b_{mn}^l / \bar{b}_n^l + \sum_{j \neq l}^{(1,L)} \sum_{\nu=1}^{N^j} \sum_{\mu=-\nu}^{\nu} (B_{mn\mu\nu}^{jl} a_{\mu\nu}^j + A_{mn\mu\nu}^{jl} b_{\mu\nu}^j) = q_{mn}^l. \tag{14b}$$

In solving the partial scattered fields, vector translation coefficients $(A_{mn\mu\nu}^{jl}, B_{mn\mu\nu}^{jl})$ play a key role. The following section reviews the analytical expressions for $A_{mn\mu\nu}^{jl}$ and $B_{mn\mu\nu}^{jl}$ used in the code gmm01f.f for their evaluation.

4. Vector translation coefficients

As formulated by Xu,[16,17] vector translation coefficients can be expressed in terms of the Gaunt coefficient,[18]

$$A_{mn\mu\nu}^{jl} = C_0 \exp\left[i(\mu - m)\varphi^{jl}\right] \sum_{q=0}^{q_{\max}} i^p C_p a_q h_p^{(1)}(kd^{jl}) P_p^{\mu-m}(\cos\vartheta^{jl}), \tag{15a}$$

$$B_{mn\mu\nu}^{jl} = C_0 \exp\left[i(\mu - m)\varphi^{jl}\right] \sum_{q=1}^{Q_{\max}} i^{p+1} b_q h_{p+1}^{(1)}(kd^{jl}) P_{p+1}^{\mu-m}(\cos\vartheta^{jl}), \tag{15b}$$

where

$$p = n + \nu - 2q, \tag{16a}$$

$$q_{\max} = \min\left[n, \nu, (n + \nu - |\mu - m|)/2\right], \tag{16b}$$

$$Q_{\max} = \min\left[n, \nu, (n + \nu + 1 - |\mu - m|)/2\right], \tag{16c}$$

$$C_0 = \frac{(-1)^m}{2} \left[\frac{(2n+1)(2\nu+1)}{n(n+1)\nu(\nu+1)} \frac{(n+m)!(\nu-\mu)!}{(n-m)!(\nu+\mu)!}\right]^{1/2}, \tag{16d}$$

$$C_p = n(n+1) + \nu(\nu+1) - p(p+1). \tag{16e}$$

Here, $(d^{jl}, \vartheta^{jl}, \varphi^{jl})$ are the spherical coordinates of the origin of the lth coordinate system (i.e., the lth sphere-center) in the jth coordinate system, $a_q = a(-m, n, \mu, \nu, p)$ is the Gaunt coefficient, and

$$b_q = \frac{2p+3}{A_{p+2}} \left[(p+2)(p_1+1)\alpha_{p+1} a_q - (p+1)(p_2+2)\alpha_{p+2} a_{q-1} \right], \quad A_{p+2} \neq 0, \tag{17a}$$

$$\begin{aligned} b_q =& \frac{2p+3}{(p+3)(p_1+2)A_{p+4}} \\ & \times \{ [A_{p+3}A_{p+4} + (p+2)(p+4)(p_1+3)(p_2+3)\alpha_{p+3}] a_{q-1} \\ & \quad - (p+2)(p+3)(p_2+3)(p_2+4)\alpha_{p+4} a_{q-2} \}, \qquad A_{p+2} = 0, \end{aligned} \tag{17b}$$

$$A_p = -p(p-1)(m+\mu) + (m-\mu)(n-\nu)(n+\nu+1), \tag{17c}$$

$$p_1 = p + m - \mu, \tag{17d}$$

$$p_2 = p - m + \mu, \tag{17e}$$

$$\alpha_p = \frac{[p^2 - (n-\nu)^2][p^2 - (n+\nu+1)^2]}{(4p^2-1)}. \tag{17f}$$

When $A_{p+2} = A_{p+4} = 0$, i.e., A_p vanishes independently of the value of p, $B^{jl}_{mn\mu\nu} = 0$. This includes the cases: (i) $\mu = m = 0$ and (ii) $\mu = -m$ and $\nu = n$. In addition, $B^{jl}_{mn\mu\nu} = 0$ when (i) $m = n$ and $\mu = -\nu$ and (ii) $m = -n$ and $\mu = \nu$. Also, in the following cases the expression for b_q is rather simple:
(i) $q = 1$,

$$b_1 = \frac{(2p+3)A_{p+3}}{(p+3)(p_1+2)}, \tag{18}$$

(ii) $q = q_{\max}$ and $n + \nu - 2q_{\max} = |n - \nu|$ or $|m + \mu|$,

$$b_{q_{\max}} = -\frac{(2p+3)A_{p+1}}{p(p_2+1)} a_{q_{\max}}, \tag{19}$$

(iii) $q = q_{\max} + 1$, $n + \nu - 2q_{\max} = |m + \mu| + 1$ and $A_{p+2} \neq 0$,

$$b_{q_{\max}+1} = -\frac{(2p+3)(p+1)(p_2+2)\alpha_{p+2}}{A_{p+2}} a_{q_{\max}}. \tag{20}$$

Equations (15a) and (15b), the explicit expressions for $A^{jl}_{mn\mu\nu}$ and $B^{jl}_{mn\mu\nu}$, involve a single set of Gaunt coefficients $a_q = a(-m, n, \mu, \nu, p)$. Note the negative sign in front of m. It is clear from Eqs. (15) that an efficient evaluation of $A^{jl}_{mn\mu\nu}$ and $B^{jl}_{mn\mu\nu}$ relies on an accurate and expeditious computation of Gaunt coefficients. Xu[17,20] has obtained convenient recurrence formulae for Gaunt coefficients, which are highly desirable in practical calculations. These recurrence relations are reviewed in the following section.

In practical scattering calculations, there is a very useful numerical scheme developed by Mackowski[6] for translating wave-expansion vectors between displaced coordinate systems. Mackowski's three-step (rotation-translation-rotation) technique is able to evade the computation of vector translation coefficients in general case by decomposition of $A^{jl}_{mn\mu\nu}$ and $B^{jl}_{mn\mu\nu}$ into rotational and axial translational parts. The code gmm01f.f uses Mackowski's three-step procedure for the expansion-vector translation process and involves in practical calculations only the translation along z axis. In the special case of translating wave-expansion vectors along z axis, the expressions for vector translation coefficients become much simpler than the general form, Eqs. (15). In this particular case, $A^{jl}_{mn\mu\nu}$ and $B^{jl}_{mn\mu\nu}$ exist only when $m = \mu$. For a translation in the positive z direction ($\cos\theta^{jl} = 1$),

$$A^{jl}_{mnm\nu} = C_0 \sum_{q=0}^{\min(n,\nu)} i^p C_p a_q h_p^{(1)}(kd^{jl}), \tag{21a}$$

$$B^{jl}_{mnm\nu} = C_0 \sum_{q=1}^{\min(n,\nu)} i^{p+1} b_q h_{p+1}^{(1)}(kd^{jl}), \tag{21b}$$

and in the negative z direction ($\cos\theta^{jl} = -1$),

$$A^{jl}_{mnm\nu} = (-1)^{n+\nu} C_0 \sum_{q=0}^{\min(n,\nu)} i^p C_p a_q h_p^{(1)}(kd^{jl}), \tag{22a}$$

$$B^{jl}_{mnm\nu} = -(-1)^{n+\nu} C_0 \sum_{q=1}^{\min(n,\nu)} i^{p+1} b_q h_{p+1}^{(1)}(kd^{jl}). \tag{22b}$$

In the case of axial translation, the Gaunt coefficients involved are $a(-m, n, m, \nu, p)$ only.

5. Recurrence formulae of Gaunt coefficients

The Gaunt coefficient is defined by[18]

$$a(s, n, \mu, \nu, p) = \frac{(2p+1)}{2} \frac{(p-s-\mu)!}{(p+s+\mu)!} \int_{-1}^{1} P_n^s(x) P_\nu^\mu(x) P_p^{s+\mu}(x) \mathrm{d}x. \tag{23}$$

An alternative definition for Gaunt coefficients is[19]

$$P_n^s(x) P_\nu^\mu(x) = \sum_{q=0}^{q_{\max}} a_q P_p^{s+\mu}(x), \tag{24}$$

where $p = n + \nu - 2q$, $a_q = a(s, n, \mu, \nu, p)$, and $q_{\max} = \min[n, \nu, (n + \nu - |s + \mu|)/2]$. As derived by Xu,[17,20] Gaunt coefficients have the following three-term recurrence relation,

$$c_0 a_q = c_1 a_{q-1} + c_2 a_{q-2}, \tag{25}$$

where

$$c_0 = (p+2)(p+3)(p_1+1)(p_1+2) A_{p+4} \alpha_{p+1}, \tag{26a}$$

$$\begin{aligned} c_1 = & A_{p+2} A_{p+3} A_{p+4} + (p+1)(p+3)(p_1+2)(p_2+2) A_{p+4} \alpha_{p+2} \\ & + (p+2)(p+4)(p_1+3)(p_2+3) A_{p+2} \alpha_{p+3}, \end{aligned} \tag{26b}$$

$$c_2 = -(p+2)(p+3)(p_2+3)(p_2+4) A_{p+2} \alpha_{p+4}. \tag{26c}$$

In Eqs. (26), A_p, p_1, p_2 and α_p are defined by Eqs. (17c–f), respectively, with $-m$ replaced by s. When $\mu = s$ and $\nu = n$, A_p vanishes independently of p so that the three-term relation Eq. (25) reduces to two terms:

$$(p+2)(p_1+1)\alpha_{p+1}a_q = (p+1)(p_2+2)\alpha_{p+2}a_{q-1}. \tag{27}$$

In particular, when $\mu = s = 0$, it further reduces to

$$\alpha_{p+1}a_q = \alpha_{p+2}a_{q-1}. \tag{28}$$

When $A_{p+4} = 0$ but $A_{p+6} \neq 0$, the three-term relation Eq. (25) is replaced by the following four-term recurrence formula,

$$c_0 a_q = c_1 a_{q-1} + c_2 a_{q-2} + c_3 a_{q-3}, \tag{29}$$

where

$$c_0 = (p+2)(p+3)(p+5)(p_1+1)(p_1+2)(p_1+4)A_{p+6}\alpha_{p+1}, \tag{30a}$$
$$c_1 = (p+5)(p_1+4)A_{p+6}[A_{p+2}A_{p+3} + (p+1)(p+3)(p_1+2)(p_2+2)\alpha_{p+2}], \tag{30b}$$
$$c_2 = (p+2)(p_2+3)A_{p+2}[A_{p+5}A_{p+6} + (p+4)(p+6)(p_1+5)(p_2+5)\alpha_{p+5}], \tag{30c}$$
$$c_3 = -(p+2)(p+4)(p+5)(p_2+3)(p_2+5)(p_2+6)A_{p+2}\alpha_{p+6}. \tag{30d}$$

A recursive scheme for an accurate and fast evaluation of Gaunt coefficients based on these recurrence relations has been devised by Xu[17] and used in gmm01f.f. In either backward or forward recursion, the implementation of the (three-term and four-term) recurrence relations require only one single starting value. At boundaries, any quantity of a_q with the value of q outside the range $[0, q_{\max}]$ is treated to be zero. Explicit formulae for the starting values for both backward and forward recursions in all possible cases are given in Xu.[17] The code gmm01f.f involves calculation of the Gaunt coefficients $a(-m, n, m, \nu, p)$ only. For this special group of Gaunt coefficients, the recurrence relations, Eqs. (25) or (29), reduce to[4,20]

$$\alpha_{p+1}a_q - (4m^2 + \alpha_{p+2} + \alpha_{p+3})a_{q-1} + \alpha_{p+4}a_{q-2} = 0. \tag{31}$$

6. Total scattered far-field in a single-field representation

As shown above, all individual scattered fields from component spheres in an aggregate are solved in respective sphere-centered coordinate systems. Following the solution of boundary conditions for all partial scattering coefficients, the next step is to construct a single-field representation for the total scattered field from an aggregate as a whole. This step is of vital importance for nevigating towards a complete multisphere light-scattering solution. Referring to an arbitrarily located common coordinate system, the total scattered field can also be expanded in VSWF, analogous to Eqs. (11). For example, in the primary j_0th coordinate system, the single-field expansion of the total scattered field is of the form

$$\mathbf{E}_{\rm sca} = \sum_{n=1}^{N_{\max}} \sum_{m=-n}^{n} iE_{mn}\left[a_{mn}\mathbf{N}_{mn}^{(3)}(\rho,\theta,\phi) + b_{mn}\mathbf{M}_{mn}^{(3)}(\rho,\theta,\phi)\right], \tag{32a}$$

$$\mathbf{H}_{\rm sca} = \frac{k}{\omega\mu}\sum_{n=1}^{N_{\max}} \sum_{m=-n}^{n} E_{mn}\left[b_{mn}\mathbf{N}_{mn}^{(3)}(\rho,\theta,\phi) + a_{mn}\mathbf{M}_{mn}^{(3)}(\rho,\theta,\phi)\right], \tag{32b}$$

where $N_{\max} = \max(N^j)$, $j = 1, 2, \ldots, L$. There is a very simple relation between total and partial scattering coefficients for the far field, involving only a simple phase term.[8] This is because the translation of VSWF between displaced coordinate systems has an obviously correct asymptotic form valid in the far zone:

$$\mathbf{M}^{(3)}_{mn}(\rho^l, \theta^l, \phi^l) = \exp(-ik\Delta^l)\mathbf{M}^{(3)}_{mn}(\rho, \theta, \phi), \tag{33a}$$

$$\mathbf{N}^{(3)}_{mn}(\rho^l, \theta^l, \phi^l) = \exp(-ik\Delta^l)\mathbf{N}^{(3)}_{mn}(\rho, \theta, \phi), \tag{33b}$$

where $\Delta^l = X^l \sin\theta\cos\phi + Y^l \sin\theta\sin\phi + Z^l\cos\theta$. As discussed in detail by Xu,[8] in constructing a single-field expansion for the total scattered far-field, the use of Eqs. (33), the asymptotic form of addition theorems for far-field translation, is superior to appealing to the general vector addition theorems for VSWF,

$$\mathbf{M}^{(3)}_{\mu\nu}(\rho^l, \theta^l, \phi^l) = \sum_{n=1}^{\infty}\sum_{m=-n}^{n} \frac{E_{mn}}{E_{\mu\nu}} \left[\tilde{A}^{lj_0}_{mn\mu\nu}\mathbf{M}^{(3)}_{mn}(\rho, \theta, \phi) + \tilde{B}^{lj_0}_{mn\mu\nu}\mathbf{N}^{(3)}_{mn}(\rho, \theta, \phi)\right], \tag{34a}$$

$$\mathbf{N}^{(3)}_{\mu\nu}(\rho^l, \theta^l, \phi^l) = \sum_{n=1}^{\infty}\sum_{m=-n}^{n} \frac{E_{mn}}{E_{\mu\nu}} \left[\tilde{B}^{lj_0}_{mn\mu\nu}\mathbf{M}^{(3)}_{mn}(\rho, \theta, \phi) + \tilde{A}^{lj_0}_{mn\mu\nu}\mathbf{N}^{(3)}_{mn}(\rho, \theta, \phi)\right]. \tag{34b}$$

Here, $(\tilde{A}^{lj_0}_{mn\mu\nu}, \tilde{B}^{lj_0}_{mn\mu\nu})$ are also vector translation coefficients. The only difference between $(\tilde{A}^{lj_0}_{mn\mu\nu}, \tilde{B}^{lj_0}_{mn\mu\nu})$ and $(A^{lj_0}_{mn\mu\nu}, B^{lj_0}_{mn\mu\nu})$ is the generating function, j_n for the former and $h^{(1)}_n$ for the latter. Based on Eqs. (33), the total scattering coefficients in Eqs. (32) regarding the far field are given by[8]

$$a_{mn} = \sum_{l=1}^{L} \exp(-ik\Delta^l) a^l_{mn}, \qquad b_{mn} = \sum_{l=1}^{L} \exp(-ik\Delta^l) b^l_{mn}, \tag{35}$$

which do not involve general addition theorems represented by Eqs. (34) and leave vector translation coefficients $(\tilde{A}^{lj_0}_{mn\mu\nu}, \tilde{B}^{lj_0}_{mn\mu\nu})$ out. It is worth emphasizing that a_{mn} and b_{mn} given above in Eqs. (35) are angular-dependent because Δ^l varies with θ and ϕ. This brings distinct features to the theoretical description of radiative multiparticle-scattering.

7. Amplitude scattering matrix

A rigorous analytical representation of the amplitude scattering matrix of an aggregate of particles is pivotal in developing a complete multiparticle scattering formulation. It allows to formulate all fundamental aggregate-scattering properties analytically. Explicit expressions for the amplitude scattering matrix of an aggregate of spheres are first discussed by Xu.[7] The formulae are later revised based on the far-field solution to multisphere scattering.[8]

According to van de Hulst[21] and Bohren and Huffman,[22] for a z-propagating incident plane wave, the relation between incident and scattered amplitudes in far zone can be conveniently written in the matrix form

$$\begin{bmatrix} E_{\|\mathrm{sca}} \\ E_{\perp\mathrm{sca}} \end{bmatrix} = \frac{\exp[ik(r-z)]}{-ikr} \begin{bmatrix} S_2 & S_3 \\ S_4 & S_1 \end{bmatrix} \begin{bmatrix} E_{\|\mathrm{inc}} \\ E_{\perp\mathrm{inc}} \end{bmatrix}, \tag{36}$$

where $(E_{\|\mathrm{inc}}, E_{\perp\mathrm{inc}})$ and $(E_{\|\mathrm{sca}}, E_{\perp\mathrm{sca}})$ are, respectively, the incident field and the scattered far-field components, parallel and perpendicular to the scattering plane that is defined by the z axis, i.e., the incident direction, and the scattering direction. For the multisphere-scattering case under consideration, the incident amplitudes are

$$E_{\|\mathrm{inc}} = E_0 \cos(\phi - \beta_{\mathrm{p}}) \exp(ikz), \qquad E_{\perp\mathrm{inc}} = E_0 \sin(\phi - \beta_{\mathrm{p}}) \exp(ikz), \tag{37}$$

and the four elements of the amplitude scattering matrix are given by[7,8]

$$\begin{aligned} S_2(\theta,\phi) = {} & \sum_{l=1}^{L} \exp(-ik\Delta^l) \sum_{n=1}^{N^l} \sum_{m=0}^{n} \frac{1}{1+\delta_{0m}} \\ & \times \{\Psi_{mn}^l \cos[(m-1)\phi + \beta_{\mathrm{p}}] + i\Phi_{mn}^l \sin[(m-1)\phi + \beta_{\mathrm{p}}]\}, \end{aligned} \tag{38a}$$

$$\begin{aligned} S_3(\theta,\phi) = {} & \sum_{l=1}^{L} \exp(-ik\Delta^l) \sum_{n=1}^{N^l} \sum_{m=0}^{n} \frac{1}{1+\delta_{0m}} \\ & \times \{i\Phi_{mn}^l \cos[(m-1)\phi + \beta_{\mathrm{p}}] - \Psi_{mn}^l \sin[(m-1)\phi + \beta_{\mathrm{p}}]\}, \end{aligned} \tag{38b}$$

$$\begin{aligned} S_4(\theta,\phi) = {} & \sum_{l=1}^{L} \exp(-ik\Delta^l) \sum_{n=1}^{N^l} \sum_{m=0}^{n} \frac{1}{1+\delta_{0m}} \\ & \times \{-i\Theta_{mn}^l \cos[(m-1)\phi + \beta_{\mathrm{p}}] + \Xi_{mn}^l \sin[(m-1)\phi + \beta_{\mathrm{p}}]\}, \end{aligned} \tag{38c}$$

$$\begin{aligned} S_1(\theta,\phi) = {} & \sum_{l=1}^{L} \exp(-ik\Delta^l) \sum_{n=1}^{N^l} \sum_{m=0}^{n} \frac{1}{1+\delta_{0m}} \\ & \times \{\Xi_{mn}^l \cos[(m-1)\phi + \beta_{\mathrm{p}}] + i\Theta_{mn}^l \sin[(m-1)\phi + \beta_{\mathrm{p}}]\}. \end{aligned} \tag{38d}$$

In Eqs. (38a–d), δ_{0m} is the Krönecker delta symbol,

$$\Psi_{mn}^l = a_{mn}^l \tilde{\tau}_{mn} + b_{mn}^l \tilde{\pi}_{mn} + (-1)^m (a_{-mn}^l \tilde{\tau}_{mn} - b_{-mn}^l \tilde{\pi}_{mn}), \tag{39a}$$

$$\Phi_{mn}^l = a_{mn}^l \tilde{\tau}_{mn} + b_{mn}^l \tilde{\pi}_{mn} - (-1)^m (a_{-mn}^l \tilde{\tau}_{mn} - b_{-mn}^l \tilde{\pi}_{mn}), \tag{39b}$$

$$\Theta_{mn}^l = a_{mn}^l \tilde{\pi}_{mn} + b_{mn}^l \tilde{\tau}_{mn} - (-1)^m (a_{-mn}^l \tilde{\pi}_{mn} - b_{-mn}^l \tilde{\tau}_{mn}), \tag{39c}$$

$$\Xi_{mn}^l = a_{mn}^l \tilde{\pi}_{mn} + b_{mn}^l \tilde{\tau}_{mn} + (-1)^m (a_{-mn}^l \tilde{\pi}_{mn} - b_{-mn}^l \tilde{\tau}_{mn}), \tag{39d}$$

where $\tilde{\pi}_{mn}$ and $\tilde{\tau}_{mn}$ are normalized angular functions, $\tilde{\pi}_{mn} = C_{mn}\pi_{mn}$ and $\tilde{\tau}_{mn} = C_{mn}\tau_{mn}$, with $C_{mn} = i^{-n} E_{mn}/E_0$, i.e.,

$$C_{mn} = \left[\frac{(2n+1)}{n(n+1)} \frac{(n-m)!}{(n+m)!} \right]^{1/2}. \tag{40}$$

Convenient recurrence relations for $\tilde{\pi}_{mn}$ and $\tilde{\tau}_{mn}$ are similar to and can be easily derived from those for π_{mn} and τ_{mn}. It is worthwhile to mention that the formulae given above are for a single polarization state of the incident plane wave with an arbitrary linear polarization angle β_{p}. A conventional definition of the amplitude scattering matrix is

$$\mathbf{S} = \begin{bmatrix} S_2^{\|} & S_3^{\perp} \\ S_4^{\|} & S_1^{\perp} \end{bmatrix}, \tag{41}$$

where the two elements of S_2 and S_4 are associated with the linear polarization state of the incident plane wave of $\beta_{\rm p}=\phi$ and the remaining elements, S_3 and S_1, are with $\beta_{\rm p}=\phi+90°$. Accordingly, the four elements of the amplitude scattering matrix are

$$S_2^{\|}(\theta,\phi)=\sum_{l=1}^{L}\exp(-ik\Delta^l)\sum_{n=1}^{N^l}\sum_{m=0}^{n}\frac{1}{1+\delta_{0m}}\left[\Psi_{mn}^{l(\phi)}\cos(m-1)\phi+i\Phi_{mn}^{l(\phi)}\sin(m-1)\phi\right], \tag{42a}$$

$$S_4^{\|}(\theta,\phi)=-\sum_{l=1}^{L}\exp(-ik\Delta^l)\sum_{n=1}^{N^l}\sum_{m=0}^{n}\frac{1}{1+\delta_{0m}}\left[i\Theta_{mn}^{l(\phi)}\cos(m-1)\phi-\Xi_{mn}^{l(\phi)}\sin(m-1)\phi\right], \tag{42b}$$

$$S_3^{\perp}(\theta,\phi)=-\sum_{l=1}^{L}\exp(-ik\Delta^l)\sum_{n=1}^{N^l}\sum_{m=0}^{n}\frac{1}{1+\delta_{0m}}\left[i\Phi_{mn}^{l(\phi+90°)}\sin(m-1)\phi+\Psi_{mn}^{l(\phi+90°)}\cos(m-1)\phi\right], \tag{42c}$$

$$S_1^{\perp}(\theta,\phi)=-\sum_{l=1}^{L}\exp(-ik\Delta^l)\sum_{n=1}^{N^l}\sum_{m=0}^{n}\frac{1}{1+\delta_{0m}}\left[\Xi_{mn}^{l(\phi+90°)}\sin(m-1)\phi-i\Theta_{mn}^{l(\phi+90°)}\cos(m-1)\phi\right], \tag{42d}$$

where $\Psi_{mn}^{l(\phi)}$, $\Phi_{mn}^{l(\phi)}$, $\Theta_{mn}^{l(\phi)}$, and $\Xi_{mn}^{l(\phi)}$ are given by Eqs. (40a–d) in terms of $a_{mn}^{l(\phi)}$, $b_{mn}^{l(\phi)}$, $a_{-mn}^{l(\phi)}$, and $b_{-mn}^{l(\phi)}$ solved in Eqs. (14) for $\beta_{\rm p}=\phi$, and the similar for the case of $\beta_{\rm p}=\phi+90°$.

Note that the definition for the amplitude matrix used in the gmm01f code and all other gmm fixed-orientation codes is slightly different from the one described above. In the definition of van de Hulst and Bohren & Huffman, both $(E_{\|{\rm sca}}, E_{\perp{\rm sca}})$ and $(E_{\|{\rm inc}}, E_{\perp{\rm inc}})$ refer to the same scattering plane. For the amplitude matrix used in all gmm fixed-orientation codes, however, $(E_{\|{\rm inc}}, E_{\perp{\rm inc}})$ are defined with respect to the x-z plane only, which is much more convenient in practical calculations [see Ref. 23 for details].

8. Total and differential cross sections

Based on the rigorous solution to the amplitude scattering matrix, analytical expressions for all other fundamental scattering properties have been derived.[8–10]

A. Scattering cross section and asymmetry parameter

Xu[9] has shown that the total and differential scattering cross sections, $C_{\rm sca}$ and $C_{\rm sca}^l$, of an aggregate of spheres are given by

$$C_{\rm sca}=\sum_{l=1}^{L}C_{\rm sca}^l=\frac{4\pi}{k^2}\sum_{l=1}^{L}\sum_{n=1}^{N^l}\sum_{m=-n}^{n}{\rm Re}\left[a_{mn}^{l*}a_{mn}^{(l)}+b_{mn}^{l*}b_{mn}^{(l)}\right], \tag{43}$$

where

$$a_{mn}^{(l)}=\sum_{j=1}^{L}\sum_{\nu=1}^{N^j}\sum_{\mu=-\nu}^{\nu}\left(\tilde{A}_{mn\mu\nu}^{jl}a_{\mu\nu}^{j}+\tilde{B}_{mn\mu\nu}^{jl}b_{\mu\nu}^{j}\right), \tag{44a}$$

$$b_{mn}^{(l)}=\sum_{j=1}^{L}\sum_{\nu=1}^{N^j}\sum_{\mu=-\nu}^{\nu}\left(\tilde{A}_{mn\mu\nu}^{jl}b_{\mu\nu}^{j}+\tilde{B}_{mn\mu\nu}^{jl}a_{\mu\nu}^{j}\right). \tag{44b}$$

Note that $\tilde{A}^{ll}_{mn\mu\nu} = \delta_{m\mu}\delta_{n\nu}$ and $\tilde{B}^{ll}_{mn\mu\nu} \equiv 0$. Also, $a^{(t)l}_{mn}$ and $b^{(t)l}_{mn}$ are quite different from the total scattering coefficients a^{t}_{mn} and b^{t}_{mn} expanded at the center of sphere l [see Eqs. 32]. The asymmetry parameter $\overline{\cos\theta}$ of an aggregate of spheres is similarly given by[9]

$$\overline{\cos\theta} = \frac{4\pi}{k^2 C_{\mathrm{sca}}} \sum_{l=1}^{L} \sum_{n=1}^{N^l} \sum_{m=-n}^{n} \mathrm{Re}\left[a^{l*}_{mn}\tilde{a}^{(l)}_{mn} + b^{l*}_{mn}\tilde{b}^{(l)}_{mn}\right], \tag{45}$$

where

$$\tilde{a}^{(l)}_{mn} = f_1 b^{(l)}_{mn} + f_2 a^{(l)}_{mn+1} + f_3 a^{(l)}_{mn-1}, \tag{46a}$$

$$\tilde{b}^{(l)}_{mn} = f_1 a^{(l)}_{mn} + f_2 b^{(l)}_{mn+1} + f_3 b^{(l)}_{mn-1}, \tag{46b}$$

$$f_1 = \frac{m}{n(n+1)}, \tag{46c}$$

$$f_2 = \frac{1}{n+1}\left[\frac{n(n+2)(n-m+1)(n+m+1)}{(2n+1)(2n+3)}\right]^{1/2}, \tag{46d}$$

$$f_3 = \frac{1}{n}\left[\frac{(n-1)(n+1)(n-m)(n+m)}{(2n-1)(2n+1)}\right]^{1/2}. \tag{46e}$$

B. Extinction cross section

The total extinction cross section of an aggregate is given by[8, 10]

$$C_{\mathrm{ext}} = \sum_{l=1}^{L} C^l_{\mathrm{ext}} = \frac{4\pi}{k^2} \sum_{l=1}^{L} \sum_{n=1}^{N^l} \sum_{m=-n}^{n} \mathrm{Re}\left(p^{l*}_{mn} a^l_{mn} + q^{l*}_{mn} b^l_{mn}\right), \tag{47}$$

where C^l_{ext} is the contribution of the lth component, i.e., the differential extinction cross section of the lth component sphere. For the case of a z-propagating incident plane wave,

$$\begin{aligned} C_{\mathrm{ext}} = {} & \frac{2\pi}{k^2}\mathrm{Re}\sum_{l=1}^{L} \exp(-ikZ^l) \sum_{n=1}^{N^l} \sqrt{2n+1} \\ & \times\Big[\left(a^l_{1n} + b^l_{1n}\right)\exp(i\beta_{\mathrm{p}}) - \left(a^l_{-1n} - b^l_{-1n}\right)\exp(-i\beta_{\mathrm{p}})\Big]. \end{aligned} \tag{48}$$

In particular, for the two typical polarization states of the incident plane wave, $\beta_{\mathrm{p}} = 0°$ (x-polarized) and $\beta_{\mathrm{p}} = 90°$ (y-polarized), the corresponding extinction cross sections are

$$C^{(0°)}_{\mathrm{ext}} = \frac{2\pi}{k^2}\mathrm{Re}\sum_{l=1}^{L} \exp(-ikZ^l) \sum_{n=1}^{N^l} \sqrt{2n+1}\left[a^{l(0°)}_{1n} + b^{l(0°)}_{1n} - a^{l(0°)}_{-1n} + b^{l(0°)}_{-1n}\right], \tag{49a}$$

$$C^{(90°)}_{\mathrm{ext}} = \frac{2\pi}{k^2}\mathrm{Re}\sum_{l=1}^{L} i\exp(-ikZ^l) \sum_{n=1}^{N^l} \sqrt{2n+1}\left[a^{l(90°)}_{1n} + b^{l(90°)}_{1n} + a^{l(90°)}_{-1n} - b^{l(90°)}_{-1n}\right]. \tag{49b}$$

Absorption cross sections can simply be calculated by $C_{\mathrm{abs}} = C_{\mathrm{ext}} - C_{\mathrm{sca}}$. Nevertheless, C_{abs} has also been explicitly formulated[6, 8] and the three cross sections C_{ext}, C_{sca}, and C_{abs} can thus be computed independently. The difference between the two numerical results of C_{abs} can be served as a check on the accuracy of the numerical scattering solution.

C. Back-Scattering cross section

For a z-propagating incident plane wave, the back-scattering cross section is defined as

$$C_{\mathrm{bak}} = \frac{4\pi}{k^2}\left|S(\theta = 180°)\right|^2, \tag{50}$$

where $S(180°) = S_1(180°) = -S_2(180°)$. Because $\pi_{mn}(-1)$ and $\tau_{mn}(-1)$ exist only when $|m| = 1$, $\pi_{1n}(-1) = (-1)^{n+1}n(n+1)/2$, and $\tau_{1n}(-1) = -\pi_{1n}(-1)$, Eqs. (38-40) imply that

$$\begin{aligned} S(180°) =& \frac{1}{2}\sum_{l=1}^{L}\sum_{n=1}^{N^l}(-1)^{n+1}\sqrt{2n+1}\exp(ikZ^l) \\ &\times\Big[\left(a^l_{1n} - b^l_{1n}\right)\exp(i\beta_{\mathrm{p}}) - \left(a^l_{-1n} + b^l_{-1n}\right)\exp(-i\beta_{\mathrm{p}})\Big], \end{aligned} \tag{51}$$

from which the total and differential back-scattering cross sections of aggregated spheres can be readily obtained.

9. T-matrix formulation

The multisphere scattering solution GMM summarized above can be presented in an alternative form of T-matrix formulation.[15] The linear equations set up by boundary conditions, Eqs. (14), can be written in the compact matrix form, $\mathbf{A}\mathbf{a} = \mathbf{P}$, where $\mathbf{a} = \left[a^l_{mn}, b^l_{mn}\right]^{\mathrm{T}}$, $\mathbf{P} = \left[p^l_{mn}, q^l_{mn}\right]^{\mathrm{T}}$, and $\mathbf{A} = \left[\mathbf{A}^{lj}\right]$, $l, j = 1, 2, \ldots, L$, $1 \le n \le N^l$, $|m| \le n$. $\mathbf{A}$ is a square matrix. Its inverse $\mathbf{T} = \mathbf{A}^{-1}$ is the particle-centered aggregate T-matrix. The entire solution of GMM rests directly on $\mathbf{T}$.

A. Amplitude scattering matrix

All equations for the amplitude scattering matrix elements remain unchanged except that the partial scattering coefficients in Eqs. (40) are now given in terms of the particle-centered aggregate T-matrix,

$$\begin{aligned} a^l_{sn} = \frac{1}{2}\sum_{\nu=1}^{N_{\max}}\sqrt{2\nu+1}\Big[&\left(T^{l11}_{sn1\nu} + T^{l12}_{sn1\nu} - T^{l11}_{sn,-1\nu} + T^{l12}_{sn,-1\nu}\right)\cos\beta_{\mathrm{p}} \\ &- \left(T^{l11}_{sn1\nu} + T^{l12}_{sn1\nu} + T^{l11}_{sn,-1\nu} - T^{l12}_{sn,-1\nu}\right)i\sin\beta_{\mathrm{p}}\Big], \end{aligned} \tag{52a}$$

$$\begin{aligned} b^l_{sn} = \frac{1}{2}\sum_{\nu=1}^{N_{\max}}\sqrt{2\nu+1}\Big[&\left(T^{l21}_{sn1\nu} + T^{l22}_{sn1\nu} - T^{l21}_{sn,-1\nu} + T^{l22}_{sn,-1\nu}\right)\cos\beta_{\mathrm{p}} \\ &- \left(T^{l21}_{sn1\nu} + T^{l22}_{sn1\nu} + T^{l21}_{sn,-1\nu} - T^{l22}_{sn,-1\nu}\right)i\sin\beta_{\mathrm{p}}\Big], \end{aligned} \tag{52b}$$

where $N_{\max} = \max(N^j)(j = 1, 2, \ldots, L)$ as given earlier and

$$T^{lpq}_{sn\mu\nu} = \sum_{j=1}^{L}\exp(ikZ^j)T^{jlpq}_{sn\mu\nu}, \tag{53}$$

which implies that $T^{jlpq}_{sn\mu\nu} = 0$ when $\nu > N^j$. In particular, for the two typical incident polarizations $\beta_{\rm p} = 0°$ or $90°$, Eqs. (52) become

$$a^{l(0°)}_{sn} = \frac{1}{2}\sum_{\nu=1}^{N_{\max}} \sqrt{2\nu+1}\left(T^{l11}_{sn1\nu} + T^{l12}_{sn1\nu} - T^{l11}_{sn,-1\nu} + T^{l12}_{sn,-1\nu}\right), \tag{54a}$$

$$b^{l(0°)}_{sn} = \frac{1}{2}\sum_{\nu=1}^{N_{\max}} \sqrt{2\nu+1}\left(T^{l21}_{sn1\nu} + T^{l22}_{sn1\nu} - T^{l21}_{sn,-1\nu} + T^{l22}_{sn,-1\nu}\right), \tag{54b}$$

$$a^{l(90°)}_{sn} = -\frac{i}{2}\sum_{\nu=1}^{N_{\max}} \sqrt{2\nu+1}\left(T^{l11}_{sn1\nu} + T^{l12}_{sn1\nu} + T^{l11}_{sn,-1\nu} - T^{l12}_{sn,-1\nu}\right), \tag{54c}$$

$$b^{l(90°)}_{sn} = -\frac{i}{2}\sum_{\nu=1}^{N_{\max}} \sqrt{2\nu+1}\left(T^{l21}_{sn1\nu} + T^{l22}_{sn1\nu} + T^{l21}_{sn,-1\nu} - T^{l22}_{sn,-1\nu}\right). \tag{54d}$$

In practical calculations, $\mathbf{T}^l$ matrices ($T^{lpq}_{nn\mu\nu}$) for all l can also be directly computed without the calculation of $\mathbf{T}$, the sphere-centered aggregate T-matrix ($T^{jlpq}_{mn\mu\nu}$). This can be done through the same interation procedure used in solving the boundary condition equations for partial scattering coefficients a^l_{mn} and b^l_{mn}.

B. Cross sections

$$\begin{aligned}C_{\rm ext} = \frac{\pi}{k^2}\mathrm{Re}\sum_{l=1}^{L}\sum_{n=1}^{N^l}\sum_{\nu=1}^{N_{\max}}\sum_{p=1}^{2}\sum_{q=1}^{2}&\sqrt{(2n+1)(2\nu+1)}\exp(-ikZ^l)\\ \times\Big\{&T^{lpq}_{1n1\nu} + (-1)^q T^{lpq}_{1n,-1\nu}\exp(i2\beta_{\rm p})\\ &+(-1)^p\left[T^{lpq}_{-1n1\nu}\exp(-i2\beta_{\rm p}) + (-1)^q T^{lpq}_{-1n,-1\nu}\right]\Big\}.\end{aligned} \tag{55}$$

$$\begin{aligned}C_{\rm sca} = \frac{\pi}{k^2}\mathrm{Re}\sum_{l=1}^{L}\sum_{n=1}^{N^l}\sum_{m=-n}^{n}\sum_{\nu=1}^{N_{\max}}\sum_{\nu'=1}^{N_{\max}}\sum_{p=1}^{2}\sum_{q=1}^{2}\sum_{q'=1}^{2}&\left[(2\nu+1)(2\nu'+1)\right]^{1/2}\\ \times\Big\{T^{lpq*}_{mn1\nu}&\left[T^{(t)lpq'}_{mn1\nu'} + \exp(i2\beta_{\rm p})(-1)^{q'}T^{(t)lpq'}_{mn,-1,\nu'}\right]\\ &+(-1)^q T^{lpq*}_{mn,-1\nu}\left[\exp(-i2\beta_{\rm p})T^{(t)lpq'}_{mn1\nu'} + (-1)^{q'}T^{(t)lpq'}_{mn,-1\nu'}\right],\end{aligned} \tag{56}$$

$$\begin{aligned}\overline{\cos\theta} = \frac{\pi}{k^2 C_{\rm sca}}\mathrm{Re}\sum_{l=1}^{L}\sum_{n=1}^{N^l}\sum_{m=-n}^{n}\sum_{\nu=1}^{N_{\max}}\sum_{\nu'=1}^{N_{\max}}\sum_{p=1}^{2}\sum_{q=1}^{2}\sum_{q'=1}^{2}&\left[(2\nu+1)(2\nu'+1)\right]^{1/2}\\ \times\Big\{T^{lpq*}_{mn1\nu}&\left[\tilde{T}^{(t)lpq'}_{mn1\nu'} + \exp(i2\beta_{\rm p})(-1)^{q'}\tilde{T}^{(t)lpq'}_{mn,-1,\nu'}\right]\\ &+(-1)^q T^{lpq*}_{mn,-1\nu}\left[\exp(-i2\beta_{\rm p})\tilde{T}^{(t)lpq'}_{mn1\nu'} + (-1)^{q'}\tilde{T}^{(t)lpq'}_{mn,-1\nu'}\right],\end{aligned} \tag{57}$$

where

$$T_{mn\mu\nu}^{(t)lpq} = \sum_{l'=1}^{L} \sum_{n'=1}^{N^{l'}} \sum_{m'=-n'}^{n'} \left[\tilde{A}_{mnm'n'}^{l'l} T_{m'n'\mu\nu}^{l'pq} + \tilde{B}_{mnm'n'}^{l'l} T_{m'n'\mu\nu}^{l'(3-p)q} \right], \tag{58a}$$

$$\tilde{T}_{mn\mu\nu}^{(t)lpq} = f_1 T_{mn\mu\nu}^{(t)l(3-p)q} + f_2 T_{m,n+1,\mu\nu}^{(t)lpq} + f_3 T_{m,n-1,\mu\nu}^{(t)lpq} \tag{58b}$$

with f_1, f_2, f_3 defined by Eqs. (46).

$$\begin{aligned} C_{\text{bak}} = \sum_{l=1}^{L} C_{\text{bak}}^{l} = \frac{\pi}{4k^2} \text{Re} & \sum_{l=1}^{L} \sum_{n=1}^{N^l} \sum_{\nu=1}^{N_{\max}} \sum_{l'=1}^{L} \sum_{n'=1}^{N^{l'}} \sum_{\nu'=1}^{N_{\max}} \sum_{p=1}^{2} \sum_{q=1}^{2} \sum_{p'=1}^{2} \sum_{q'=1}^{2} \\ & (-1)^{n+n'} \left[(2n+1)(2n'+1)(2\nu+1)(2\nu'+1)\right]^{1/2} \exp\left(ikZ^{ll'}\right) \\ & \times \left\{ (-1)^{p+1} \left[T_{1n1\nu}^{lpq*} + (-1)^q T_{1n,-1\nu}^{lpq*} \exp(-i2\beta_{\text{p}}) \right] \right. \\ & \qquad \left. - \left[T_{-1n1\nu}^{lpq*} \exp(i2\beta_{\text{p}}) + (-1)^q T_{-1n,-1\nu}^{lpq*} \right] \right\} \\ & \times \left\{ (-1)^{p'+1} \left[T_{1n'1\nu'}^{l'p'q'} + (-1)^{q'} T_{1n',-1\nu'}^{l'p'q'} \exp(i2\beta_{\text{p}}) \right] \right. \\ & \qquad \left. - \left[T_{-1n'1\nu'}^{l'p'q'} \exp(-i2\beta_{\text{p}}) + (-1)^{q'} T_{-1n',-1\nu'}^{l'p'q'} \right] \right\}. \end{aligned} \tag{59}$$

In the multisphere-scattering T-matrix formulation given above, a single-centered aggregate T-matrix $\mathbf{T}^{\text{t}}$ can be derived as

$$\begin{aligned} T_{mn\mu\nu}^{\text{t}pq} &= \sum_{l=1}^{L} \exp\left(-ik\Delta^l\right) T_{mn\mu\nu}^{lpq} \\ &= \sum_{l=1}^{L} \sum_{j=1}^{L} \exp\left[i\left(\mathbf{k}\cdot\mathbf{d}^j - k\Delta^l\right)\right] T_{mn\mu\nu}^{jlpq}. \end{aligned} \tag{60}$$

Both $\mathbf{T}^l$ and $\mathbf{T}^{\text{t}}$ include the incident phase term and thus vary with incident direction. Consequently, $\mathbf{T}^l$ and $\mathbf{T}^{\text{t}}$ are not the T-matrix in the normal sense. Only the particle-centered T-matrix $\mathbf{T}$ is independent of incident field.

10. Practical examples for using code gmm01f.f

This section provides practical examples for testing the multisphere-scattering code gmm01f.f. Each example includes input and output files, laboratory scattering measurements for i_{11} and i_{22} (the dimensionless polarized scattered intensities as a function of scattering angle), and a figure showing the comparison of theoretical calculation results with the experimental data of i_{11} and i_{22}. In scattering calculations, $i_{11} = |S_1|^2$ and $i_{22} = |S_2|^2$, where S_1 and S_2 are the amplitude scattering matrix elements. Most of the experimental data are obtained using the modern w-band microwave scattering facility at the Laboratory for Astrophysics, University of Florida.[24,25]

Example 1

This example refers to two identical optical glass BK7 spheres in contact.[26] Size parameter of each component sphere is 7.86 and the refractive index of the spheres is (2.5155,0.0213). The orientation of this bisphere system is such that the axis of symmetry of the two spheres is parallel to the scattering plane and perpendicular to the incident plane wave vector. Figure 1 shows the comparison of i_{11} and i_{22} between theoretical calculation results from gmm01f.f and laboratory scattering measurements for this simple aggregate of spheres.

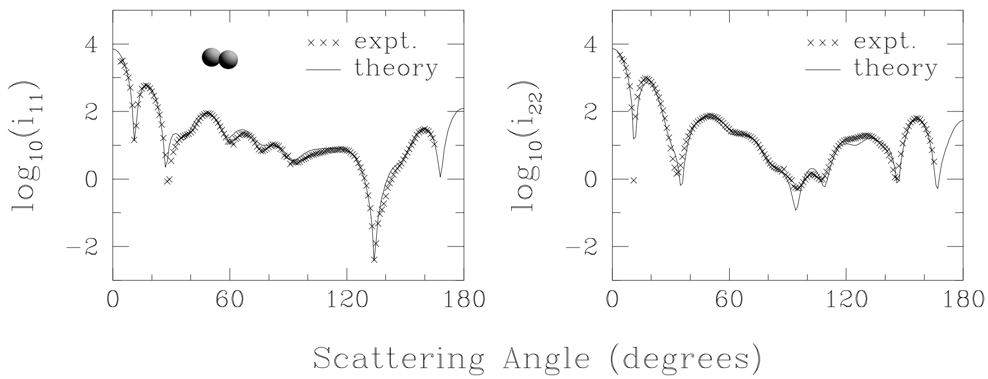

Figure 1: Comparison between laboratory scattering measurements ("expt.") and theoretical solutions ("theory") for i_{11} and i_{22} of an aggregate of two idential optical glass BK7 spheres in a single orientation.

A sample file of gmm01f.par for compiling the code:

parameter (nLp=2,np=20).

Two input files, all output files, and the two experimental data files for i_{11} and i_{22} are in **exam01.data**.

Example 2

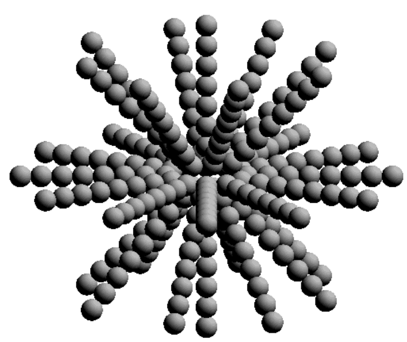

Figure 2: An aggregate of 240 identical nylon spheres (see Zerull *et al.* 1993).

Shown in this example is an aggregate of 240 identical nylon spheres, configured like a "Christmas star". An individual sphere has the size parameter of 0.58 and refractive index of (1.735,0.007). In 1989, Zerull *et al.*[27] measured the scattering of this 240-sphere aggregate at an average over azimuthal angles (i.e., an average over orientations when the aggregate

rotates about its axis perpendicular to the scattering plane), using a microwave scattering facility at Bochum, Germany. Figure 3 compares theoretical predictions with the laboratory data obtained by Zerull *et al.* for the averaged i_{11} and i_{22} of the 240-sphere aggregate.
A sample file of gmm01f.par for compiling the code:

parameter (nLp=240,np=4).

The two input files, all output files, and the two experimental data files for i_{11} and i_{22} are in **exam02.data**.

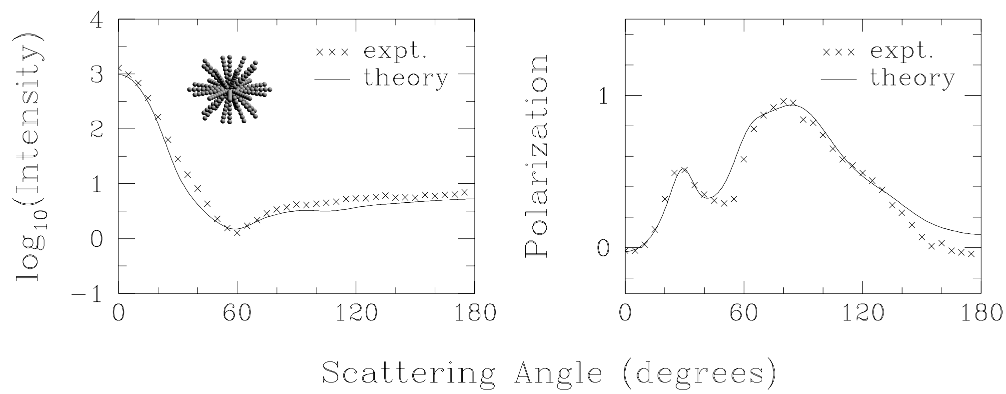

Figure 3: Comparison between theoretical solutions ("theory") and laboratory scattering measurements ("expt.") for azimuthal-averaged i_{11} and i_{22} of the aggregate of 240 identical nylon spheres. The experimental data were obtained by Zerull *et al.* in 1989.

Example 3

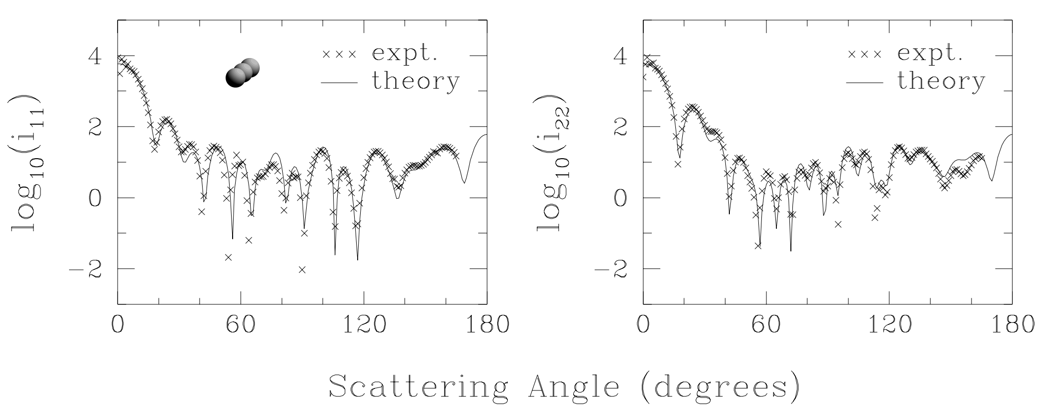

Figure 4: Comparison between theoretical predictions and laboratory microwave scattering measurements for the angular distributions of i_{11} and i_{22} of a linear chain of three acrylic spheres.

This example is for a linear chain consisting of three touching identical acrylic spheres. Each component sphere has the size parameter of 7.49 and refractive index of (1.615,0.008). The orientation of this three-sphere chain is such that its axis of symmetry is along the direction of propagation of the incident plane wave. Figure 4 shows the comparison between computed and measured i_{11} and i_{22} for this aggregate of three spheres.

A sample file of gmm01f.par for compiling the code:

parameter (nLp=3,np=20).

The two input files, all output files, and the two experimental data files for i_{11} and i_{22} are in **exam03.data**.

Example 4

This example refers to an aggregate of nine identical acrylic spheres that form a 3×3 square array. Its orientation is such that the square surface plane is parallel to the scattering plane and its two sides are perpendicular to the direction of propagation of the incident radiation. Each component sphere has the size parameter of 5.03 and refractive index of (1.615,0.008). Figure 5 is the comparison between theory and experiment for i_{11} and i_{22} of this square array of nine spheres.

A sample file of gmm01f.par for compiling the code:

parameter (nLp=9,np=15)

The two input files, all output files, and the two experimental data files for i_{11} and i_{22} are in **exam04.data**.

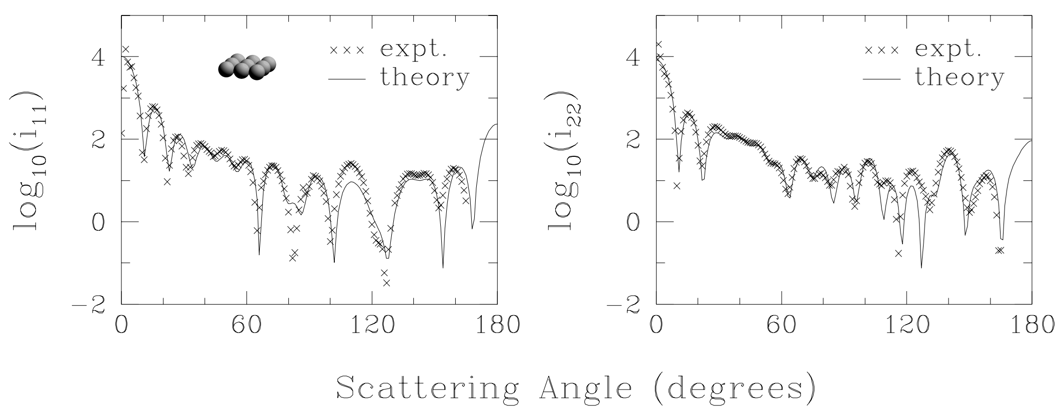

Figure 5: Comparison of computed i_{11} and i_{22} with laboratory scattering measurements for a 3×3 square array of nine acrylic spheres.

Example 5

In this example is a two-layer rectangular aggregate of eighteen identical acrylic spheres. Each of the two layers is a 3×3 square sphere-array. The top and bottom square surface planes are parallel to the scattering plane and the two pairs of sides are, respectively, parallel and perpendicular to the direction of propagation of the incident plane wave. Each component sphere has the size parameter of 5.03 and refractive index of (1.615,0.008).

A sample file of gmm01f.par for compiling the code:

parameter (nLp=18,np=15).

The two input files, all output files, and the two experimental data files for i_{11} and i_{22} are in **exam05.data**.

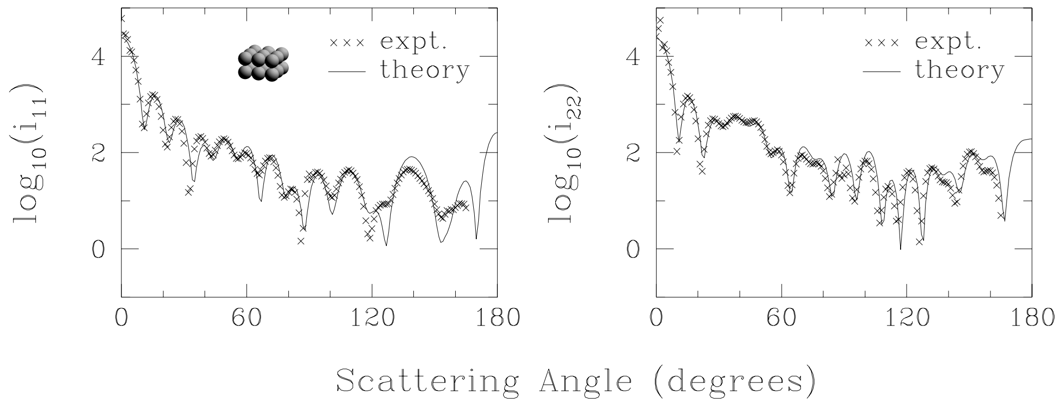

Figure 6: Comparison of the computed i_{11} and i_{22} from gmm01f.f with laboratory scattering measurements for a 18-sphere aggregate.

Example 6

In this example is a pyramid-like aggregate of fourteen identical acrylic spheres. The 3×3 square bottom of the pyramid is parallel to the scattering plane and the two pairs of the square sides are parallel and perpendicular to the incident direction, respectively. Component spheres are the same as in examples 4 and 5.

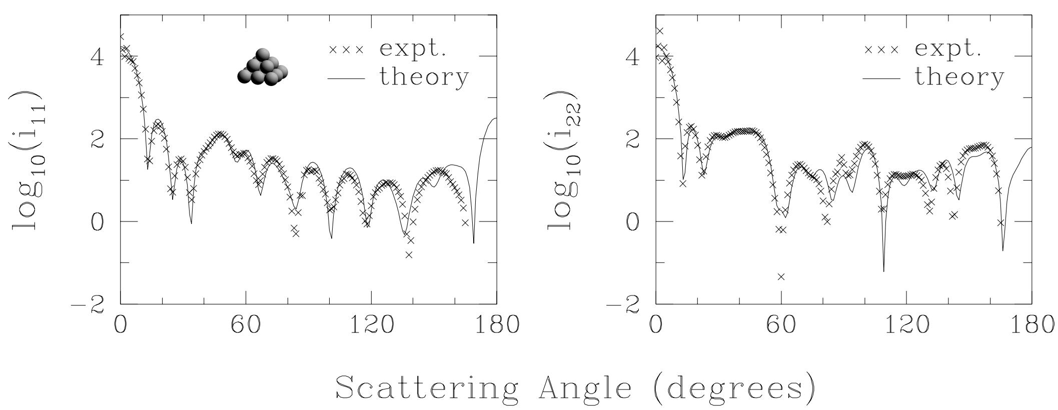

Figure 7: Comparison of the computed i_{11} and i_{22} from gmm01f.f with laboratory scattering measurements for a 25-sphere square array.

A sample file of gmm01f.par for compiling the code:

```
parameter (nLp=14,np=15)
```

The two input files, all output files, and the two experimental data files for i_{11} and i_{22} are in **exam06.data**.

Example 7

This example shows a 5×5 square sphere-array. The 25 component spheres are identical and the same as in examples 4–6.

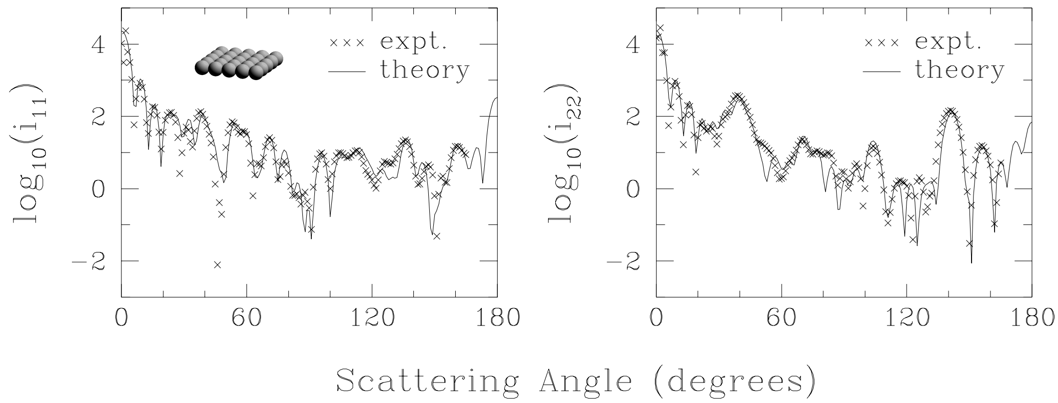

Figure 8: Comparison of the computed i_{11} and i_{22} from gmm01f.f with laboratory scattering measurements for the 18-sphere aggregate in example 5.

A sample file of gmm01f.par for compiling the code:

parameter (nLp=25,np=15).

The two input files, all output files, and the two experimental data files for i_{11} and i_{22} are in **exam07.data**.

Example 8

This example refers to an aggregate of 32 acrylic spheres, which has a 5-sphere linear chain on the top, a 6×2 rectangular array in the middle, and a 5×3 rectangular array at the bottom. The bottom plane of the aggregate is parallel to the scattering plane and the longer sides of the two rectangular arrays and the axis of symmetry of the top linear chain are perpendicular to the incident plane wave vector.

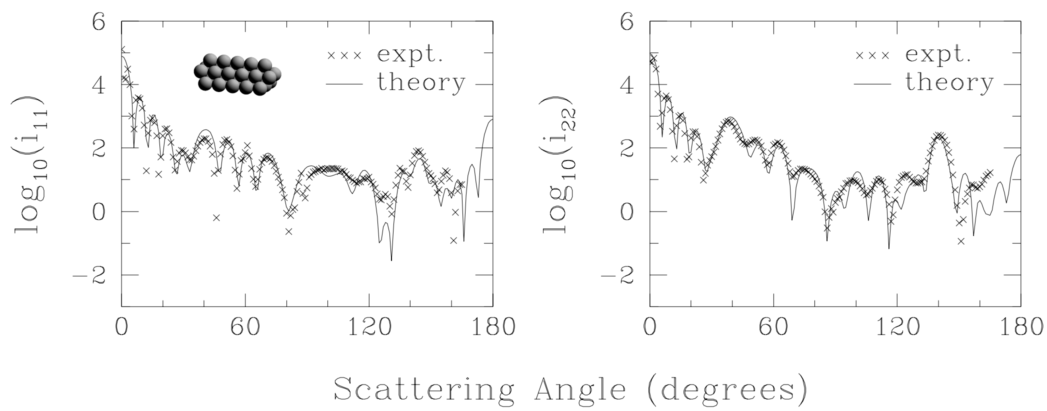

Figure 9: Comparison of the computed i_{11} and i_{22} from gmm01f.f with laboratory scattering measurements for a 32-sphere aggregate.

A sample file of gmm01f.par for compiling the code:

parameter (nLp=32,np=15).

The input and output files and the experimental data of i_{11} and i_{22} are in **exam08.data**.

Example 9_1

This example refers to an aggregate of an aggregate of fifteen spheres. The configuration of this aggregate is such that three identical 3/8" optical BK7 glass spheres are on top of a 6×2 rectangle bottom of twelve 1/4" acrylic spheres. The axes of symmetry of the top three BK7 spheres and the two linear chains of six acrylic spheres are along the incident direction and parallel to the scattering plane of $\phi = 0°$. The 6×2 rectangle bottom of the aggregate has a 3.5° tilt angle with the scattering plane. All neighboring spheres are in contact.

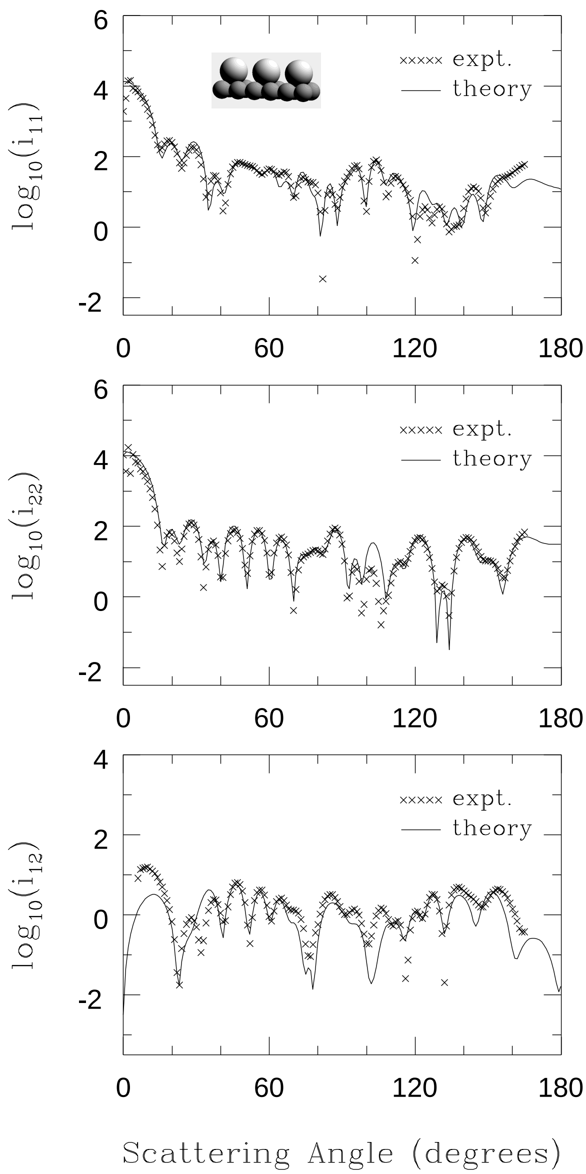

Figure 10: Comparison between theoretical and experimental results for a fifteen-sphere aggregate. The top three identical spheres have an individual size parameter of 7.49 and refractive index of (2.5155,0.0213). The bottom twelve identical spheres have an individual size parameter of 5.03 and refractive index of (1.615,0.008).

The two input and all output files as well as the laboratory scattering measurement data for i_{11}, i_{22}, and i_{12} are in **exam09_1.data**.

Example 9_2

This is the same aggregate in the above example 9_1 except that the 15-sphere aggregate is rotated in the scattering plane by 45°.

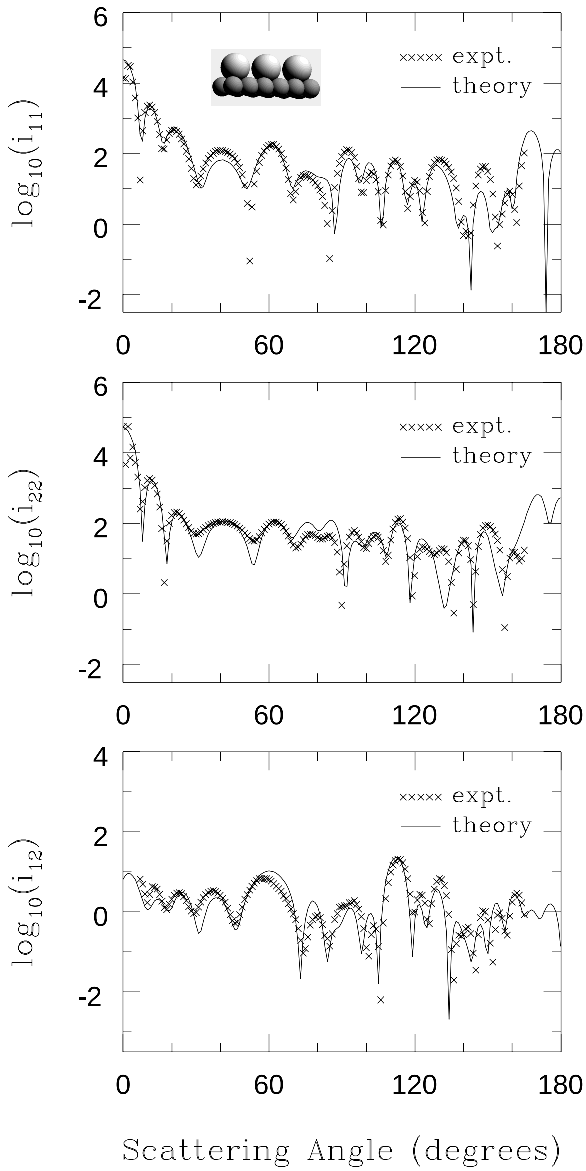

Figure 11: Comparison of the theoretical results of i_{11}, i_{22}, and i_{12} with laboratory scattering measurements for the 15-sphere aggregate in example9_1 after a rotation in the scattering plane by 45°.

The input and output files as well as the experimental data are in **exam09_2.data**.

11. Internal field distributions

This code includes also the calculation of the three-dimensional distributions of internal fields inside component spheres, which has been discussed in detail in Ref. 11.

References

[1] S. Stein, "Addition theorems for spherical wave functions," Q. Appl. Math. **19,** 15–24 (1961).

[2] O. R. Cruzan, "Translational addition theorems for spherical vector wave functions," Q. Appl. Math. **20,** 33–40 (1962).

[3] C. Liang and Y. T. Lo, "Scattering by two spheres," Radio Sci. **2**, 1481–1495 (1967).

[4] J. H. Bruning and Y. T. Lo, "Multiple scattering of EM waves by spheres, part I & II," IEEE Trans. Anten. Prop. **AP-19**, 378–400 (1971).

[5] K. A. Fuller and G. W. Kattawar, "Consummate solution to the problem of classical electromagnetic scattering by ensembles of spheres. I & II," Opt. Lett. **13,** 90–92; 1063–1065 (1988).

[6] D. W. Mackowski, "Analysis of radiative scattering for multiple sphere configurations," Proc. R. Soc. London Ser. A **433**, 599–614 (1991).

[7] Y.-l. Xu, "Electromagnetic scattering by an aggregate of spheres," Appl. Opt. **34**, 4573–4588 (1995); errata, ibid. **37**, 6494 (1998).

[8] Y.-l. Xu, "Electromagnetic scattering by an aggregate of spheres: far field," Appl. Opt. **36**, 9496–9508 (1997).

[9] Y.-l. Xu, "Electromagnetic scattering by an aggregate of spheres: asymmetry parameter," Phys. Lett. A **249**, 30–36 (1998).

[10] Y.-l. Xu and R. T. Wang, "Electromagnetic scattering by an aggregate of spheres: Theoretical and experimental study of the amplitude scattering matrix," Phys. Rev. E **58**, 3931–3948 (1998).

[11] Y.-l. Xu, B. Å. S. Gustafson, F. Giovane, J. Blum, S. Tehranian, "Calculation of the heat-source function in photophoresis of aggregated spheres," Phys. Rev. E **60**, 2347–2365 (1999).

[12] L. V. Lorenz, "Sur la Lumière réfléchie et réfractée par une sphère transparente," in *Oeuvres Scientifiques de L. Lorenz,* revues et annotées par H. Valentiner (Librairie Lehman et Stage, Copenhagen, 1898), pp. 405–529.

[13] G. Mie, "Beiträge zur Optik trüber Medien speziell Kolloidaler Metallösungen," Ann. Phys. Leipzig **25**, 377–452 (1908).

[14] P. Debye, "Der Lichtdruck auf Kugeln von beliebigem Material," Ann. Phys. Leipzig **30**, 57–136 (1909).

[15] Y.-l. Xu and B. Å. S. Gustafson, "A generalized multiparticle Mie-solution: Further experimental verification," JQSRT **70**, 395–419 (2001).

[16] Y.-l. Xu, "Calculation of the addition coefficients in electromagnetic multisphere-scattering theory," J. Comput. Phys. **127**, 285–298 (1996); erratum, ibid. **134**, 200 (1997).

[17] Y.-l. Xu, "Efficient evaluation of vector translation coefficients in multiparticle light-scattering theories," J. Comput. Phys. **139**, 137–165 (1998).

[18] J. A. Gaunt, "On the triplets of helium," Philos. Trans. R. Soc. London Ser. A **228**, 151–196 (1929).

[19] Y.-l. Xu, "Fast evaluation of the Gaunt coefficients," Math. Comput. **65**, 1601–1612 (1996).

[20] Y.-l. Xu, "Fast evaluation of Gaunt coefficients: recursive approach," J. Comput. Appl. Math. **85**, 53–65 (1997).

[21] H. C. van de Hulst, *Light Scattering by Small Particles* (Wiley, New York, 1957).

[22] C. F. Bohren and D. R. Huffman, *Absorption and Scattering of Light by Small Particles* (Wiley, New York, 1983).

[23] Y.-l. Xu, "Scattering Mueller matrix of an ensemble of variously shaped small particles," J. Opt. Soc. Am. A **20**, 2093–2105 (2003).

[24] B. Å. S. Gustafson, "Microwave analog to light scattering measurements: a modern implementation of a proven method to achieve precise control," JQSRT **55**, 663–672 (1996).

[25] B. Å. S. Gustafson,"Microwave analog to light scattering measurements," in *Light Scattering by Nonspherical Particles*, M. I. Mishchenko, J. W. Hovenier, and L. D. Travis Eds. (Academic Press, San Diego, California, 2000), Ch. 13, pp. 367–390.

[26] Y.-l. Xu and B. Å. S. Gustafson, "Experimental and theoretical results of light scattering by aggregates of spheres," Appl. Opt. **36**, 8026–8030 (1997).

[27] R. H. Zerull, B. Å. S. Gustafson, K. Schulz, and E. Thiele-Corbach, "Scattering by aggregates with and without an absorbing mantle: microwave analog experiments," Appl. Opt. **32**, 4088–4100 (1993).